Available online at www.sciencedirect.com
SCIENCE DIRECT®
International Journal of Thermal Sciences 43 (2004) 1153–1160
International Journal of Thermal Sciences
www.elsevier.com/locate/ijts

Numerical investigation on mixed convection in a non-Newtonian fluid inside a vertical duct

G. Lorenzini [a], C. Biserni [b,*]

[a] *Dipartimento di Ingegneria Agraria, Università degli Studi di Bologna, Viale Fanin 50, 40127 Bologna, Italy*
[b] *Dipartimento di Ingegneria Energetica, Nucleare e del Controllo Ambientale, Università degli Studi di Bologna, Viale Risorgimento 2, 40136 Bologna, Italy*

Received 15 July 2003; received in revised form 1 April 2004; accepted 1 April 2004

Available online 17 June 2004

Abstract

This paper reports a numerical study of the thermal and fluid-dynamic behaviour of laminar mixed convection in a non-Newtonian fluid inside a vertical duct enclosed within two vertical plates that are plane and parallel, having linearly varying wall temperatures. The other inlet conditions consist of a parabolic distribution of the velocity field and a constant fluid temperature. The problem is assumed to be steady and two-dimensional. The formulation of a mathematical model in dimensionless co-ordinates and the discretisation of the governing equations by means of the finite difference method, have made it possible to create a numerical code developed in Matlab environment. The study was focused on the simultaneous presence and on the mutual interaction of natural and forced convection, starting from the effects of the re-circulation on the heat transfer. The quantitative results of the analysis, which are strongly affected by the variation of the Grashof number and of the exponent of the power law, are given in terms of graphic visualisations of the fluid velocity profiles and, when the governing parameters vary, of the various geometries characterising the heat transfer.

Keywords: Mixed convection; Grashof number; Re-circulation; Non-Newtonian fluid; Finite difference method

1. Introduction

Combined forced and free convection (mixed convection flow) is encountered in many technical and industrial applications, which include solar central receivers exposed to the wind currents, electronic devices cooled by fans, nuclear reactors cooled during emergency shutdown and (especially for the dynamic inlet conditions here adopted) heat exchangers placed in low-velocity-environments. Various recent researches on mixed convection are significant with particular reference to the above-mentioned industrial applications: in [1] a study of mixed convection heat and mass transfer along a vertical wavy surface has been carried out numerically. Ref. [2] deals with a procedure for rapidly estimating the flow-rate and heat transfer for laminar free and mixed convection in inclined ducts. The problem becomes more difficult when it is unsteady [3], or in the case of a porous medium [4]. Mixed convection problems have been widely studied: going ahead to the beginning of the 1960's, researchers began to undertake studies in geometrical conditions similar to the ones considered here, regarding solutions of forced convection [5], completely developed mixed convection [6] or cases [7,8] that questioned the one-directionality of the flow, neglecting the effects of the buoyancy forces. In many applications, the effects of natural convection, again associated with the presence of temperature gradients, may be compared to those of forced convection. This is why it is necessary to introduce a criterion of evaluation capable of quantifying the contribution of both mechanisms. In Refs. [9,10], for instance, the following criteria are suggested:

(1) $Pr = 1$ fixed, an estimate of the ratio between the effect of natural and forced convection is given by the value of Gr/Re^2:

* Corresponding author.
E-mail address: cesare.biserni@mail.ing.unibo.it (C. Biserni).

1290-0729/$ – see front matter
doi:10.1016/j.ijthermalsci.2004.04.005

Nomenclature

Bo	Boussinesq number	x	transversal co-ordinate ..... m
d	half-width of the duct ..... m	X	non-dimensional transversal co-ordinate
f	friction factor	y	axial co-ordinate ..... m
g	gravitational acceleration ..... $m{\cdot}s^{-2}$	Y	non-dimensional axial co-ordinate
Gr	Grashof number	*Greek symbols*	
H	size of the mesh pitch in transversal direction m	α	thermal molecular diffusion coefficient of the fluid ..... $m^2{\cdot}s^{-1}$
K	size of the mesh pitch in axial direction ..... m	β	thermal expansion coefficient of the fluid . K^{-1}
n	power-law index	θ	non-dimensional temperature
$N_{x,y}$	number of grid points in the transversal and axial direction	Ψ	non-dimensional stream function
NNN	length of the duct expressed in half-width units	Ω	non-dimensional vorticity
Nu	Nusselt number	*Subscripts*	
Pr	Prandtl number	i	transversal direction
Re	Reynolds number	j	axial direction
T	fluid temperature ..... K	m	average value
$\mathbf{V}$	fluid velocity vector	0	boundary values
u	transversal component of velocity ..... $m{\cdot}s^{-1}$	w	wall
U	transversal component of the non-dimensional velocity	∞	values for $y \to \infty$

- $Gr/Re^2 \ll 1 \Rightarrow$ the buoyancy forces are negligible in comparison to the ones of inertia and therefore the mechanism of forced convection is prevailing;
- $Gr/Re^2 \approx 1 \Rightarrow$ the motion is affected to the same extent by the two types of forces and therefore the convection is mixed;
- $Gr/Re^2 \gg 1 \Rightarrow$ the preponderant influence of the buoyancy forces makes the effects deriving from the accumulative motion of the fluid negligible and therefore natural convection appears to prevail.

(2) $Pr > 1$, an estimate of the ratio between the effect of natural and forced convection is given by the value of $Ra_y^{1/4}/(Re_y^{1/2}Pr^{1/3})$:
- $Ra_y^{1/4}/(Re_y^{1/2}Pr^{1/3}) < O(1) \Rightarrow$ Forced convection;
- $Ra_y^{1/4}/(Re_y^{1/2}Pr^{1/3}) > O(1) \Rightarrow$ Natural convection.

(3) $Pr < 1$, an estimate of the ratio between the effect of natural and forced convection is given by the value of $Bo_y^{1/4}/Pe_y^{1/2}$:
- $Bo_y^{1/4}/Pe_y^{1/2} < O(1) \Rightarrow$ Forced convection;
- $Bo_y^{1/4}/Pe_y^{1/2} > O(1) \Rightarrow$ Natural convection.

The Eckert–Diaguila diagram [11] defines a representation of the different fluid-dynamic combinations with the respective field of influence of the types of convection. When making progress with research and consequently with the formulation of increasingly complex mathematical models, the need to validate experimentally the results obtained was considered of primary importance. In this context is included the numerical and experimental analysis [12] in which the heat transfer is considered in a mixed convection regime of air flow between two parallel plates that are uniformly heated. Correlations related to Nu are proposed with reference to the region in which the flow is fully developed, in correspondence to the establishment of the secondary flow and to the zone in which a first increase in heat transfer is detected (which clearly follows the secondary flow). In Ref. [13], the problem of convective heat transfer in laminar motion, although limited to the region in which the motion is fully developed, is generalised to the case of a vertical channel to which heat is asymmetrically exchanged. Different combinations, consisting of the fact that the two walls are characterised alternatively by constant thermal flux or constant temperature, are studied separately as boundary conditions. Considering the same range of boundary conditions, the above-described study is extended in Ref. [14] to the mixed convection, with reference to the inversion of velocity flow. This phenomenon is encountered whenever the Re/Gr ratio proves to be lower than a particular threshold value (a function of the boundary conditions adopted), in the region adjacent to the lower temperature wall. In Ref. [15], an analytical survey is presented on the forced convection of a fluid that flows in laminar motion inside tubes having circular shaped fins, computing the presence of such fins, in the descriptive mathematical model, with a harmonic variation of the Biot number along the duct. In Ref. [16] the study considers non-finned ducts and the determination of the geometric parameters optimising the heat transfer. In this background, the present paper presents a numerical investigation based on finite difference method, in which a power low fluid, having inlet parabolic velocity profile and constant temperature, is considered inside a vertical duct with linearly varying temperature along the channel axis direction.

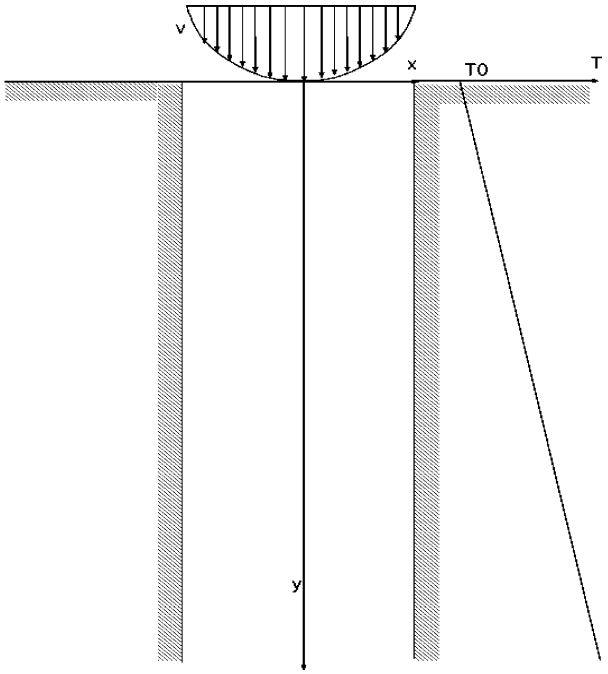

Fig. 1. Schematization of the model.

2. Description of the physical model

With reference to Fig. 1, we consider a power-law fluid in laminar flow inside a vertical duct with walls of semi-infinite length ($0 \leqslant y < \infty$; y increasing downwards) placed at a distance from the axis, which is equal to $x = +d$ and $x = -d$. An inlet parabolic velocity profile is also assumed:

$$\vec{V}_0 = (u_0, v_0) = (0, v_0) \tag{1}$$

$$v_0 = v_m\left[(-3/2)(x/d)^2 + 3/2\right] \tag{2}$$

The flow is steady and two-dimensional. The walls are assumed to have a linear variation of temperature,

$$T_w = T_0 - (\lambda/d)y \tag{3}$$

in which λ represents the constant rate of temperature change along the walls. The entrance temperature of the fluid is considered constant and equivalent to T_0:

$$T(x, 0) = T_0 \tag{4}$$

This pattern of constant inlet temperature of the cross section guarantees the absence of buoyancy forces prior to entering the channel, so that the eventual occurrence of the latter can be attributed only and exclusively to the temperature gradient along the walls.

3. Description of the mathematical model

The laws governing the phenomenon are the continuity equation, the equations of Navier–Stokes and the energy equation, in which the approximation of Boussinesq was used. Accordingly, the fluid is considered incompressible, except in the evaluation of the buoyancy terms: all the properties of the fluid are independent of temperature, except for density, which has a linear dependence. The governing equations may be expressed in the following non-dimensional form,

$$\Omega = \frac{\partial^2 \Psi}{\partial X^2} \tag{5}$$

$$\frac{\partial \Psi}{\partial X}\frac{\partial \Omega}{\partial Y} - \frac{\partial \Psi}{\partial Y}\frac{\partial \Omega}{\partial X} = \frac{\partial^2}{\partial X^2}\left(|\Omega|^{n-1}\Omega\right) - Gr\frac{\partial \theta}{\partial X} \tag{6}$$

$$Pr\left(\frac{\partial \Psi}{\partial X}\left(\frac{\partial \theta}{\partial Y} - 1\right) - \frac{\partial \Psi}{\partial Y}\frac{\partial \theta}{\partial X}\right) = \frac{\partial^2 \theta}{\partial X^2} \tag{7}$$

where

$$Pr = \frac{\nu_0}{\alpha}\left|\frac{\nu_m}{d}\right|^{n-2}\left(\frac{\nu_m}{d}\right) \tag{8}$$

$$Gr = \frac{g\beta\lambda d^{2n+1}|\nu_m|^{1-2n}\nu_m}{\nu_0^2} \tag{9}$$

Starting from the physical model examined and using the symmetry with respect to $x = 0$ and $0 \leqslant y < \infty$ typical of the geometry being considered, one can determine the boundary conditions for the non-dimensional functions. These may be expressed, with reference to the various "significant" locations, as follows:

Duct axis

$$\Psi(X = 0,\ 0 \leqslant Y < \infty) = 0 \tag{10}$$

$$\Omega(X = 0,\ 0 \leqslant Y < \infty) = 0 \tag{11}$$

$$\left.\frac{\partial \theta}{\partial X}\right|_{0,Y} = 0 \tag{12}$$

Duct entrance

$$\Psi(0 \leqslant X < 1,\ Y = 0) = \left(-\frac{1}{2}X^3 + \frac{3}{2}X\right) \tag{13}$$

$$\Omega(0 \leqslant X < 1,\ Y = 0) = -3X \tag{14}$$

$$\theta(0 \leqslant X < 1,\ Y = 0) = 0 \tag{15}$$

Duct wall

$$\Psi(X = 1,\ 0 \leqslant Y < \infty) = 1 \tag{16}$$

$$\theta(X = 1,\ 0 \leqslant Y < \infty) = 0 \tag{17}$$

$$\left.\frac{\partial \Psi}{\partial X}\right|_{1,Y} = 0 \tag{18}$$

4. Description of the numerical method

Here a procedure is defined based on the finite difference method to solve the parabolic equations with backward-differences in the direction of the flow and central differences in the cross direction. The governing equations, written with the finite difference method, take on the following form:

$$\Omega_{i,j+1} = \frac{1}{H^2}(\Psi_{i+1,j+1} - 2\Psi_{i,j+1} + \Psi_{i-1,j+1}) \tag{19}$$

$$\begin{aligned}&\frac{1}{2HK}\big[(\Psi_{i+1,j+1} - \Psi_{i-1,j+1})(\Omega_{i,j+1} - \Omega_{i,j}) \\ &\qquad - (\Omega_{i+1,j+1} - \Omega_{i-1,j+1})(\Psi_{i,j+1} - \Psi_{i,j})\big] \\ &\quad = \frac{1}{H^2}\big[|\Omega_{i+1,j+1}|^{n-1}\Omega_{i+1,j+1} - 2|\Omega_{i,j+1}|^{n-1}\Omega_{i,j+1} \\ &\qquad + |\Omega_{i-1,j+1}|^{n-1}\Omega_{i-1,j+1}\big] \\ &\qquad - \frac{Gr}{2H}(\theta_{i+1,j+1} - \theta_{i-1,j+1})\end{aligned} \tag{20}$$

$$\begin{aligned}&\frac{1}{2HK}\big[(\Psi_{i+1,j+1} - \Psi_{i-1,j+1})(\theta_{i,j+1} - \theta_{i,j}) \\ &\qquad - (\theta_{i+1,j+1} - \theta_{i-1,j+1})(\Psi_{i,j+1} - \Psi_{i,j})\big] \\ &\qquad - \frac{1}{H}(\Psi_{i+1,j+1} - \Psi_{i,j}) \\ &\quad = \frac{1}{Pr\,H^2}(\theta_{i+1,j+1} - 2\theta_{i,j+1} + \theta_{i-1,j+1})\end{aligned} \tag{21}$$

Where H and K are the pitch in the transversal and axial direction; the indexes (i, j) indicate the point of co-ordinates $[X = (i-1)H,\ Y = (j-1)K]$. Indicating with N_x the number of nodes in the X direction and N_y in the Y direction, we have $i = 1, \ldots, N_x + 1$ and $j = 1, \ldots, N_y + 1$. As far as the boundary conditions are concerned, the vorticity at $X = 1$ is evaluated by developing a Taylor series of Ω and Ψ up to the second order in the proximity of $X = 1$, just as the temperature condition at $X = 0$ is evaluated with the accuracy of $O(H^4)$, using the Taylor series for θ in the proximity of $X = 0$, thus obtaining as a final result:

$$3\theta_{1,j+1} - 4\theta_{2,j+1} + \theta_{3,j+1} = 0 \tag{22}$$

Eqs. (19)–(22), together with initial conditions and (first-kind) boundary conditions, constitute a system of $3N - 1$ equations in $3N - 1$ unknowns. Such equations have been discretised with the finite difference method at the node $j + 1$ in order to use Gauss' method of elimination: for this reason, the cross derivatives of Ψ, θ and Ω in Eqs. (20) and (21) are evaluated at the jth node rather than at the $(j + 1)$th. The term of vorticity of the power-law in the momentum equation (20) is evaluated by referring to the previous loop. The accuracy of the solution may suffer from such a procedure; however, this problem can be mitigated by reducing the number of nodes in the Y direction, and by evaluating at the same time the effect of this feature on the stability of the algorithm.

Once the equations are discretised, moving gradually ahead inside the duct, one can evaluate the variables in the $(j + 1)$th location in the flow direction, employing Gauss' elimination method. The calculation of Nu at the first pitch of the grid $(j = 1)$ requires separate mention; in fact, at the inlet of the channel, one has:

$$\left.\frac{\frac{\partial\theta}{\partial X}|_{X=1}}{\theta_{\mathrm{m}}}\right|_{Y=0} = \frac{0}{0} \tag{23}$$

This indeterminate form must be resolved in order to avoid discontinuity in the value of Nu: by using a finite difference calculation scheme, it becomes natural to use l'Hopital's rule, from which we obtain:

$$\begin{aligned}Nu_1 &= \lim(Y \to 0)\frac{\frac{\partial\theta}{\partial X}|_{X=1}}{\theta_m} \\ &= \lim(Y \to 0)\frac{\frac{\partial}{\partial Y}(\frac{\partial\theta}{\partial X}|_{X=1})}{\partial\theta_m/\partial Y}\end{aligned} \tag{24}$$

Bearing boundary conditions in mind, one obtains:

$$Nu_1 = \frac{\theta_{N,2}}{\theta_{m,2}h} = Nu_2 \tag{25}$$

This means that the numerical scheme is not capable of evaluating Nu for $0 < Y < H$; therefore, when wishing to determine its value in proximity to the entrance, it is necessary, leaving aside the convergence problems, to use a mesh with a very fine Y pitch.

5. The effect of the Grashof number and the power-law exponent

The solution of the system is an $O(H^2)$ in the entire domain, whereas at the inlet it is an $O(K)$; consequently, in order to obtain a better approximation of the input zone, one could consider decreasing the value of K. Such an operation cannot in any case be computed without reducing H at the same time with a heavy slow-down of computational time requested. This suggests two different methods for conducting the research: one could look for values of H and K as a compromise which give a good approximation in the entire domain or, as an alternative, conduct two separate analyses relative to the entrance region and the fully-developed region. In this study, an attempt will be made, within the limits of possibility, to consider both possibilities: the first to have a global vision of the phenomenon, and the second for a more detailed comparison with the results existing in literature.

The analysis of the influence of Gr was conducted while considering the value of the exponent n fixed at 0.7 (or 1); in this way, a choice was made to neglect, as a first approximation, the variation of n. This choice was made because varying n does not change the qualitative shape of the obtained curves, while it changes only the detailed numerical values. With reference to the diagrams in Figs. 2 and 3, negative values have been found for the axial velocities in the proximity to the walls for $Gr\frac{\mathrm{d}T_w}{\mathrm{d}y} < 0$ and at the centre for $Gr\frac{\mathrm{d}T_w}{\mathrm{d}y} > 0$ (because of the system chosen and in coherence with the physical model utilised, the above conditions become $Gr < 0$ and $Gr > 0$, respectively). In agreement with the necessary re-distribution of the velocity profiles (Figs. 4 and 5), for negative v values at the centre, we have positive cross-section velocity peaks, and negative peaks for positive v. The heat transfer is generally assisted by velocity inversion in the central zone, a phenomenon, in fact, that occurs in occasion of a flow increase that laps on

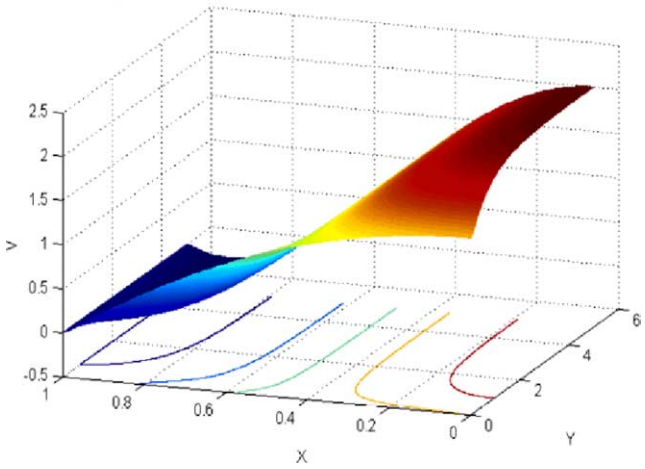

Fig. 2. Trend of the axial velocity for $Gr = -50$, $Pr = 1$, $n = 1$, $\lambda = -1$, $N_x = 100$ and $N_y = 4000$.

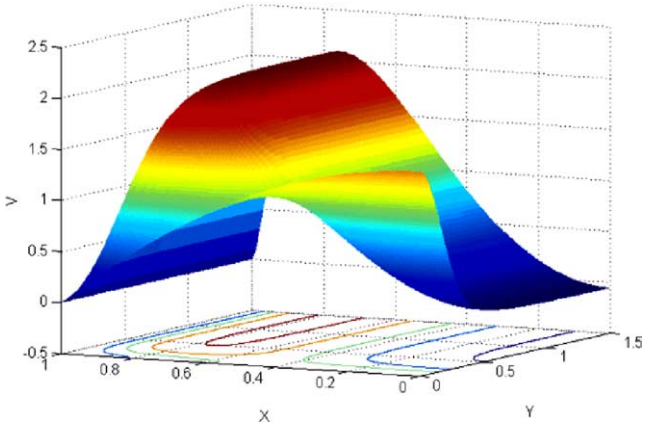

Fig. 3. Trend of the axial velocity for $Gr = 450$, $Pr = 1$, $n = 1$, $\lambda = -1$, $N_x = 100$ and $N_y = 1000$.

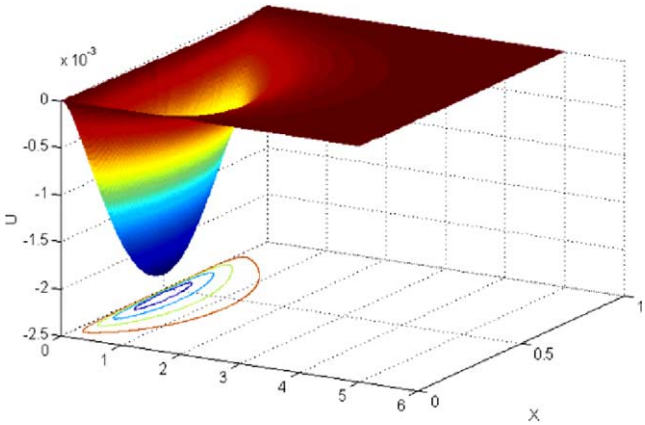

Fig. 4. Trend of the transversal velocity for $Gr = -50$, $Pr = 1$, $n = 1$, $\lambda = -1$, $N_x = 100$ and $N_y = 4000$.

the walls. This is also highlighted in the diagrams reported in Figs. 6, 7, 8 and 9, relative to the patterns, within the length of the channel expressed in equivalent diameters, of the temperature, of the non-dimensional average temperature

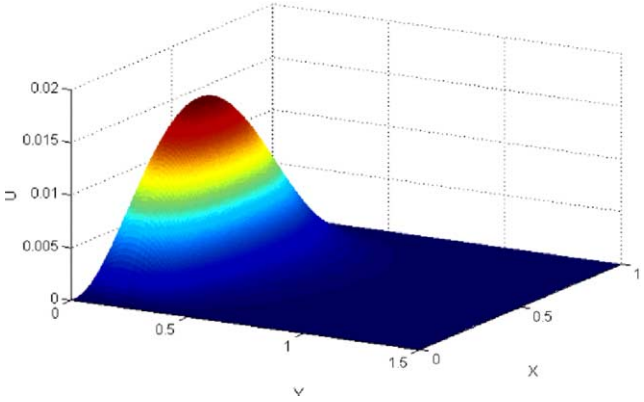

Fig. 5. Trend of the transversal velocity for $Gr = 450$, $Pr = 1$, $n = 1$, $\lambda = -1$, $N_x = 100$ and $N_y = 1000$.

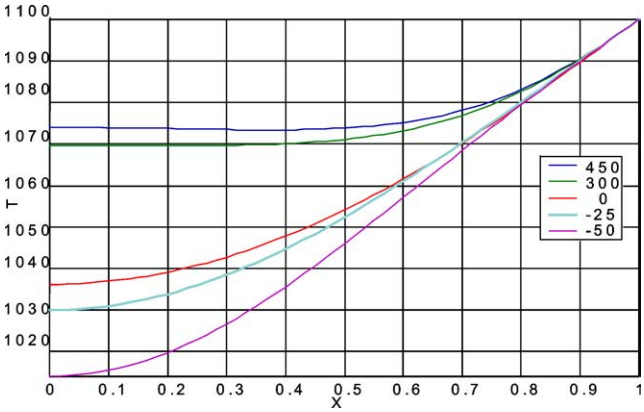

Fig. 6. Comparison, as Gr varies, of the output temperature for $Pr = 1$, $n = 0.7$, $To = 100$, $\lambda = -1$, $N_x = 60$ and $N_y = 300$.

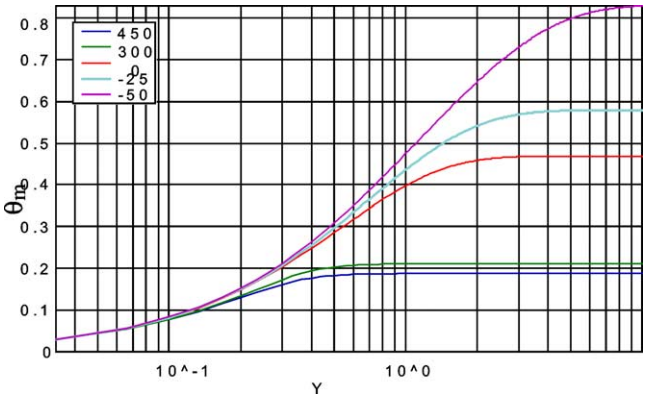

Fig. 7. Comparison, as Gr varies, of θm for $Pr = 1$, $n = 0.7$, $\lambda = -1$, $N_x = 60$ and $N_y = 300$.

θm and of Nu. The temperature proves to be higher for $Gr > 0$ on the entire section, and has a flatter pattern in the transversal direction, as well as the average non-dimensional temperature, measuring the difference of temperature of the fluid and of the wall (averaged temperature in a given section), which is constantly lower for $Gr > 0$. The indicator of the global heat transfer, Nu, takes on values that keep on growing as Gr increases. The pressure losses (Fig. 10)

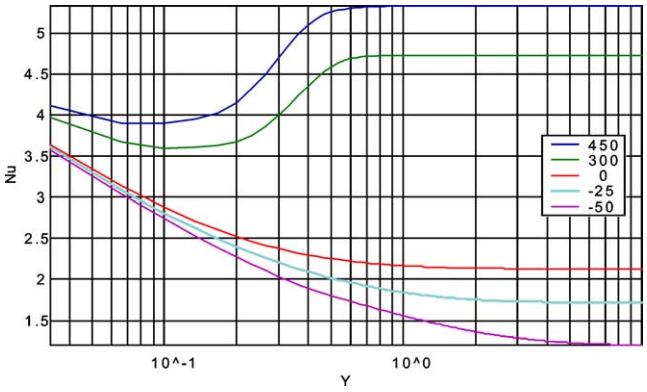

Fig. 8. Comparison, as Gr varies, of Nu for $Pr = 1$, $n = 0.7$, $\lambda = -1$, $N_x = 60$ and $N_y = 300$.

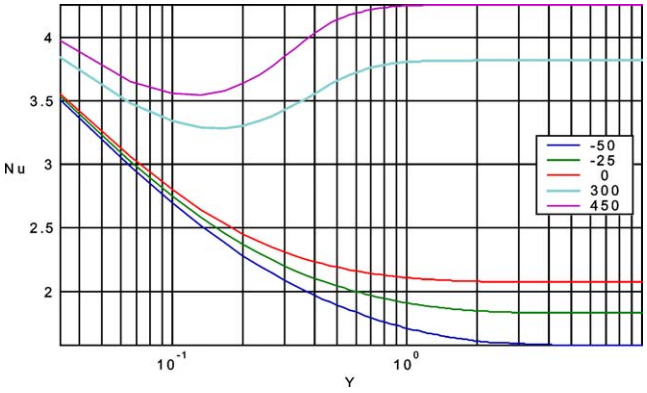

Fig. 9. Comparison, as Gr varies, of Nu for $Pr = 1$, $n = 1$, $\lambda = -1$, $N_x = 60$ and $N_y = 300$.

are analysed with reference to the friction factor f: this is affected considerably, as far as the module is concerned, by the derivative of v in transversal direction calculated on the wall, while the sign is in accordance with v.

We have analysed how the variation of the power-law exponent affects the results for two values of Gr, one higher than zero and one lower, which are equivalent to $Gr = 450$, $Gr = -50$, respectively. We did this in order to verify whether the influences of n were regardless of the sign of Gr or not. First of all, an observation must be made on the variation, generated by n, of the length of the entrance region that, as one will be able to see, will prove to be indispensable in order to establish the accuracy of the following considerations. From the analysis of the diagrams in Figs. 11 and 12 of the mean non-dimensional temperatures, which are certainly the most significant ones for establishing the depletion of the entrance region, one assumes that for decreasing n, its length tends to decrease for $Gr > 0$, and vice-versa for $Gr < 0$. With reference to the diagrams of Figs. 13 and 14, the transversal velocity gradients tend to be amplified as n decreases both for $Gr < 0$ and $Gr > 0$, generating an increase in the value (in module) of the extreme points, i.e., the points of minimum and maximum. This characteristic is confirmed

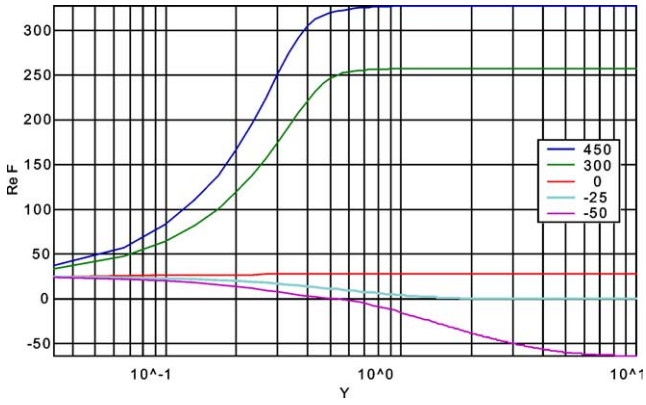

Fig. 10. Comparison, as Gr varies, of $Re \cdot f$ for $Pr = 1$, $n = 0.7$, $\lambda = -1$, $N_x = 60$ and $N_y = 300$.

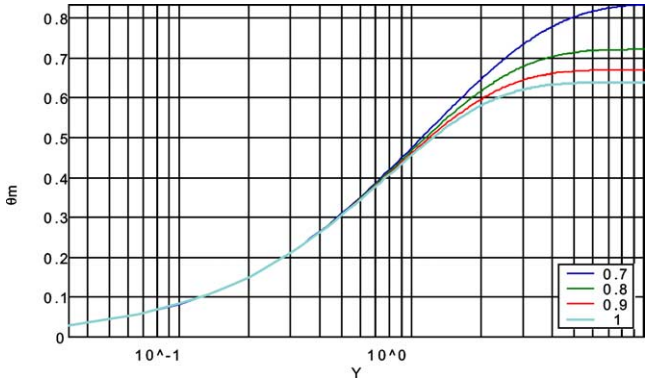

Fig. 11. Comparison, as n varies, of θm for $Gr = -50$, $Pr = 1$, $\lambda = -1$, $N_x = 80$ and $N_y = 300$.

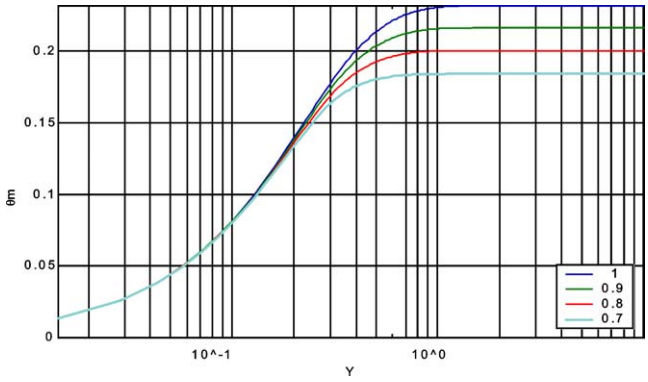

Fig. 12. Comparison, as n varies, of θm for $Gr = 450$, $Pr = 1$, $\lambda = -1$, $N_x = 200$ and $N_y = 700$.

and almost emphasised by the analysis of the other two quantities being examined: from Table 1, which synthesises the correspondences that can be deduced from the respective graphic patterns, it is shown that when n decreases, the behaviour differences between $Gr > 0$ and $Gr < 0$, relative to Nu, $Re \cdot f$, velocity and temperature, become increasingly evident.

Table 1
Table of comparison at $Y = 10$

	Nu		$Re \cdot f$		v(min)		v(max)		θm		t [°C], $X = 0$	
	Gr		Gr		Gr		Gr		Gr		Gr	
n	−50	450	−50	450	−50	450	−50	450	−50	450	−50	450
1	1.58	4.3	−18	170	−0.1	−0.04	2.2	2.07	0.64	0.17	1028	1067
0.9	1.5	4.6	−25	205	−0.18	−0.06	2.3	2.2	0.67	0.2	1025	1070
0.8	1.4	5	−37	255	−0.28	−0.09	2.5	2.3	0.72	0.215	1021	1073
0.7	1.25	5.4	−64	325	−0.51	−0.1	2.75	2.5	0.82	0.23	1015	1075

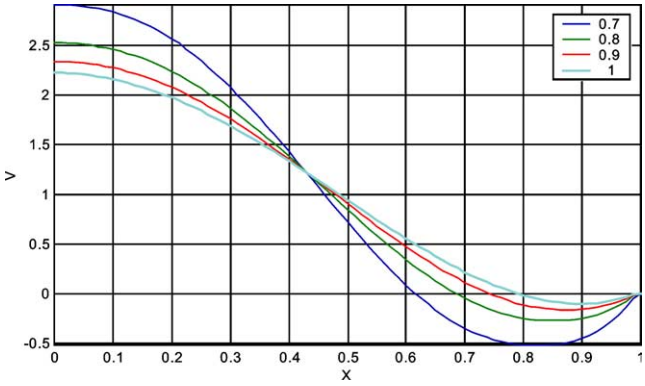

Fig. 13. Comparison, as n varies, of axial velocity for $Gr = -50$, $Pr = 1$, $\lambda = -1$, $N_x = 80$ and $N_y = 300$.

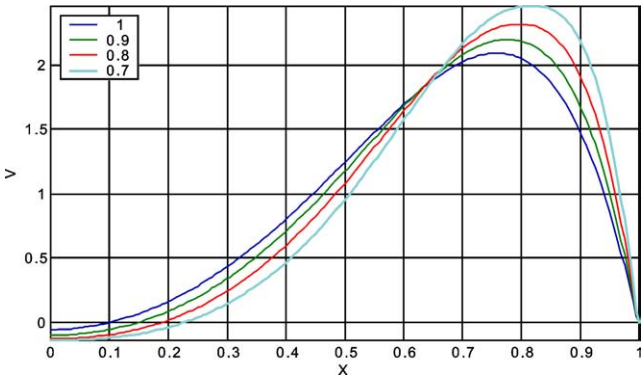

Fig. 14. Comparison, as n varies, of axial velocity for $Gr = 450$, $Pr = 1$, $\lambda = -1$, $N_x = 200$ and $N_y = 700$.

6. Conclusions and future developments

Several conclusions and ideas for future research emerged from this study. The study focused on the interaction between natural and forced convection: particular care has been posed to the effects of the re-circulation of the streamlines on the heat transfer. The Grashof number as well as the power law exponent, that have been considered separately, proved to be the parameters that greatly affect the quantitative results of the numerical investigation. The originality of the numerical scheme employed consists of its extreme simplicity and the fact that is does not need a stabilisation procedure. Moreover it is sufficiently exact with regard to the objective of this research: the results obtained in the cases presenting inverse flow zones, in the fully developed portion, match closely those obtained by other authors [17]. The work reported in this paper can be considered as a starting point for further developments in research that may regard both more detailed analyses of the results obtainable from the program and the improvement of the code as an extension of the application of the latter to more general cases. The first step to take in the direction towards a bigger versatility in the fields of use of the code is represented by the adoption of a variable grid that would avoid the problem of carrying out different analyses between the entrance region and the fully developed region, at the same time decreasing the computational load. In order to create a development hypothesis that allows for further generalisation of the problem, such as introducing in input any variation of temperature along the walls, one should not neglect a new non-dimensionalisation of the equations. One may demonstrate that the utilisation of the kernel of this code would entail, in such a case, an error in the evaluation of the energy equation, which is equivalent to:

$$\left| \frac{(T - T_w)\frac{\mathrm{d}^2 T_w}{\mathrm{d}Y^2}}{Re^2 (\frac{\mathrm{d}T_w}{\mathrm{d}Y})^2} \right| \tag{26}$$

Consequently, if the model developed should be reused without making any substantial modifications, the results would be reliable only if, for a determined trend of T_w, this factor were equivalent, in order of magnitude, to the error made by discretising the equations.

Acknowledgements

The authors wish to thank Italian MIUR for supporting this research.

References

[1] J.-H. Jang, W.-M. Yan, Mixed convection heat and mass transfer along a vertical wavy surface, Internat. J. Heat Mass Transfer 47 (2004) 419–428.
[2] B.J. Brinkworth, A procedure for the routine calculation of laminar free and mixed convection in inclined duct, Internat. J. Heat Fluid Flow 21 (2000) 456–462.
[3] R. Seshadri, N. Sreeshylan, G. Nath, Unsteady mixed convection flow in the stagnation region of a heated vertical plate due to impulsive motion, Internat. J. Heat Mass Transfer 45 (2002) 1345–1352.

[4] E.M.A. Elbashbeshy, M.A. Bazid, The mixed convection along a vertical plate with bedded in porous medium, Appl. Math. Comput. 125 (2002) 317–324.
[5] A.B. Metzner, Heat transfer in non-Newtonian fluid, Adv. Heat Transfer 2 (1965) 357–394.
[6] G.F. Scheele, T.J. Hanratty, Effect of natural convection on stability of flow in a vertical pipe, J. Fluid Mech. 14 (1962) 244–256.
[7] F. Gori, Effects of variable physical properties in laminar flow of a pseudoplastic fluid, Internat. J. Heat Mass Transfer 21 (1978) 247–250.
[8] W.J. Marner, R.A. Rehfuss, Buoyancy effects on fully-developed laminar non-Newtonian flow in a vertical tube, Chem. Engrg. J. 3 (1972) 294–300.
[9] A. Bejan, Convection Heat Transfer, second ed., Wiley, New York, 1995.
[10] A. Bejan, Heat Transfer, second ed., Wiley, New York, 1993.
[11] G. Guglielmini, C. Pisoni, Elementi di Trasmissione del Calore, Masson, Milano, 1997.
[12] J.R. Maughan, F.P. Incropera, Regions of heat transfer enhancement for laminar mixed convection in a parallel plate channel, Internat. J. Heat Mass Transfer 33 (1990) 555–570.
[13] C.-H. Cheng, H.-S. Kou, W.-H. Huang, Locally fully developed laminar free convection within asymmetrically heated vertical channel, JSME Internat. J. 33 (1990) 305–315.
[14] C.-H. Cheng, H.-S. Kou, W.-H. Huang, Flow reversal and heat transfer of fully developed mixed convection in vertical channels, J. Thermophys. 4 (1990) 375–383.
[15] C.A.C. Santos, R.M. Cotta, M.N. Ozisik, Heat transfer enhancement in laminar flow within externally finned tubes, Internat. J. Heat Technol. 9 (1991) 47–61.
[16] A. Bejan, E. Sciubba, The optimal spacing of parallel plates cooled by forced convection, Internat. J. Heat Mass Transfer 35 (1992) 3259–3264.
[17] D.B. Ingham, A.T. Jones, Combined convection flow of a power-law fluid in a vertical duct with linearly varying wall temperatures, Acta Mech. 110 (1995) 19–32.